Dopamine-Melanin Colloidal Nanospheres: An Efficient Near-Infrared Photothermal Therapeutic Agent for In Vivo Cancer Therapy

Yanlan Liu, Kelong Ai, Jianhua Liu, Mo Deng, Yangyang He, and Lehui Lu*

Cancer has overtaken heart disease and become the leading cause of death worldwide.[1,2] In 2008, approximately 7.6 million people died of cancer, and the cancer rates may further increase by 50% to 15 million new cases in the year 2020 according to the World Cancer Report. Current clinical cancer therapies are limited to surgery, radiotherapy, and chemotherapy. Unfortunately, these approaches suffer from the risks of killing normal cells, destroying the immune system, and an increased incidence of second cancers.[3–5] Owing to high selectivity and minimal invasiveness, photothermal therapy is emerging as a powerful technique for cancer treatment.[6] Its therapeutic effects occur only at the tumor sites with both photothermal therapeutic (PTT) agent accumulation and localized near-infrared (NIR) laser exposure, effectively avoiding the risks mentioned above. This technique also possesses several other potential advantages over traditional techniques, including ease of procedure, faster recovery, fewer complications, and shorter hospital stay.[7]

Currently available PTT agents mainly focus on Au-, Ag-, and Pd-based novel metal nanoparticles,[8] Cu-based semiconductor nanoparticles,[9] carbon-based nanomaterials[10] and organic polymers.[11] Despite efficient cancer therapy, these agents have not yet achieved clinical implementation, stemming from great concerns regarding their long-term safety. For instance, metallic nanoparticles are poorly biometabolized and have pertinent issues related to the safety of the metal itself, while carbon-based nanomaterials have been demonstrated to induce many toxic responses such as oxidative stress and pulmonary inflammation.[12] Developing PTT agents that consist of naturally occurring substances in organisms would be highly beneficial for in vivo applications, because it can effectively avoid serious adverse effects caused by long-term retention of foreign substances in patients, and biodegradation of these agents can also be achieved through metabolism. Nevertheless, it is hard to find such materials that intrinsically satisfy the criteria for PTT agents including strong NIR absorption and high photothermal conversion efficiency, simultaneously. To our knowledge, only one type of such material has been reported based on porphyrin-lipid as an effective in vivo PTT agent.[13] Thanks to their organic nature, the resultant porphysomes were enzymatically biodegradable and induced minimal acute toxicity during their retention in mice. With these advantages notwithstanding, we believe there is still considerable room for improvement in the synthesis and properties of PTT agents.

Melanin is a well-known biopolymer that is widely distributed in almost all living organisms and has many distinct functions, including the protection of humans and animals from ultraviolet injury, antibiotic function, thermoregulation, free radical quenching, and some nervous system involvement.[14a] Moreover, its absorption can extend to NIR regions. Inspired by this, here we present a novel PTT agent based on dopamine-melanin colloidal nanospheres (Dpa-melanin CNSs) for in vivo cancer therapy. Similar to porphysomes, Dpa-melanin CNSs were completely composed of naturally occurring Dpa-melanin yet could be easily produced with a simpler and cost-effective strategy. Benefiting from wide distribution of their component in human naturally, the as-prepared Dpa-melanin CNSs were highly superior for in vivo photothermal therapy: they showed biodegradability, a high median lethal dose, and did not induce long-term toxicity during their retention in rats. Moreover, they provided a photothermal conversion efficiency of 40%, much higher than those of previously reported PTT agents. After administration, they were able to efficiently kill tumor cells at low laser power density and short irradiation time without damaging healthy tissues. Last but not least, Dpa-melanin CNSs could be easily attached to conjugates with other interesting biofunctionalities, which provided a particularly useful platform for simultaneous diagnosis and efficient treatment of cancer.

Dpa-melanin CNSs were synthesized by the oxidation and self-polymerization of dopamine in a mixture containing water, ethanol, and ammonia at room temperature. Typical scanning electron microscopy (SEM) and transmission electron microscopy (TEM) imaging revealed that the resultant Dpa-melanin

Y. L. Liu, K. L. Ai, Prof. L. H. Lu
State Key Laboratory of Electroanalytical Chemistry
Changchun Institute of Applied Chemistry
Chinese Academy of Sciences
Changchun 130022, P.R. China
E-mail: lehuilu@ciac.jl.cn
Y. L. Liu
Graduate School of the Chinese Academy of Sciences
Beijing 100039, China
J. H. Liu
Department of Radiology
the Second Hospital of Jilin University
Changchun 130022, P.R. China
M. Deng
Department of Clinical Laboratory
the Second Hospital of Jilin University
Changchun 130022, P.R. China
Y. Y. He
Department of Pathology
the Second Hospital of Jilin University
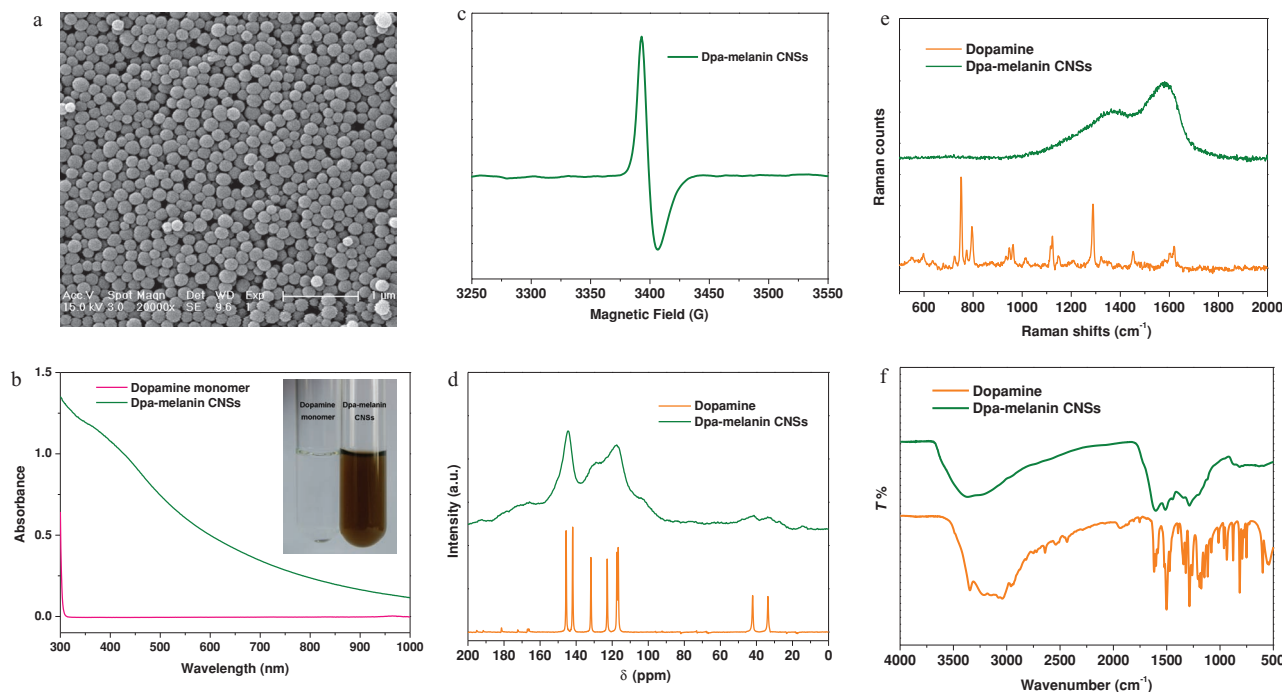Changchun 130022, P.R. China

COMMUNICATION

Figure 1. a) SEM image of Dpa-melanin CNSs. b) UV–vis absorption spectra of dopamine and Dpa-melanin CNSs. The inset shows a photograph of dopamine and Dpa-melanin CNS aqueous solutions. c) ESR spectrum of Dpa-melanin CNSs. d) ^{13}C NMR spectra. e) Raman spectra. f) FTIR spectra of dopamine and Dpa-melanin CNSs, respectively.

CNSs were spherical in shape, with an average diameter of approximately 160 nm (**Figure 1**a, Supporting Information, Figure S1). Their size could be easily controlled by tuning the molar ratio of ammonia to dopamine. For example, Dpa-melanin CNSs with an average diameter of 70 nm were obtained when the ratio was increased from 11.3 to 17 (Supporting Information, Figure S2). Nevertheless, prolonging the reaction time led to a slightly increase in the particle diameter (Supporting Information, Figure S3). Indeed, the size and morphology of the synthesized Dpa-melanin CNSs were similar to those of naturally occurring melanin, which is 40–150 nm in diameter and spherical in shape.[14b] In this work, small Dpa-melanin CNSs (70 nm) were typically used for further experiments. From the viewpoint of practical applications, small Dpa-melanin CNSs were more suitable for biological and medical fields than larger particles, because they are less likely to be rapidly recognized and cleared by phagocytes.[15a,b] They can remain in the circulation for an extended period of time, and passively accumulated in tumors through enhanced permeability and retention (EPR) effect.[15c,d] A distinct feature of naturally occurring melanin from other biopolymers is the paramagnetism because of the presence of stable π-electron free radicals.[16] Thus, electron spin resonance (ESR) of Dpa-melanin CNSs was measured to verify their successful synthesis. Similar to naturally occurring melanin, synthesized Dpa-melanin CNSs displayed a single-line ESR spectrum, and a single peak was observed with a g-factor approaching 2 (Figure 1c). This finding suggested the presence of an irregular, crosslinked polymer network with mixed bonding arrangements and radicals localized to single

quinone residues.[16] Compared with naturally occurring melanin, nevertheless, the synthesized Dpa-melanin CNSs had a sharper absorbance peak, indicating that they possessed a narrower range of bonding arrangements than naturally occurring melanin. Complementary to ESR data, solid-state ^{13}C NMR, Raman, Fourier transform infrared and X-ray photoelectron spectra, which were consistent with those of naturally occurring melanin,[17] provided additional evidence of successful melanin nanosphere synthesis (Figure 1d–f, Supporting Information, Figure S4). As prepared, Dpa-melanin CNSs dispersed well in water and remained stable for several months without any detectable agglomeration. Even after dispersal in 10% blood serum solution, hardly any change in their absorption was observed after 24 h (Supporting Information, Figure S5). This favorable colloidal stability of Dpa-melanin CNSs in aqueous media revealed their high potential for in vivo applications.

Photothermal therapy employs photosensitizing agents to generate heat from light absorption at the target sites. To avoid damaging healthy cells effectively, photosensitizing agents must have high absorption in the NIR region of the light spectrum, owing to both the deep penetration of NIR and its low absorption by tissues. Encouragingly, the synthesized Dpa-melanin CNSs exhibited broad absorption ranging from ultraviolet (UV) to NIR wavelengths relative to dopamine monomer, coupled with a color change of the solution from colorless to deep brown (Figure 1b, Supporting Information, Figure S6). The appearance of the absorption in the UV region of the light spectrum was attributed to the oxidation of dopamine into dopachrome and dopaindole, and the following self-polymerization process
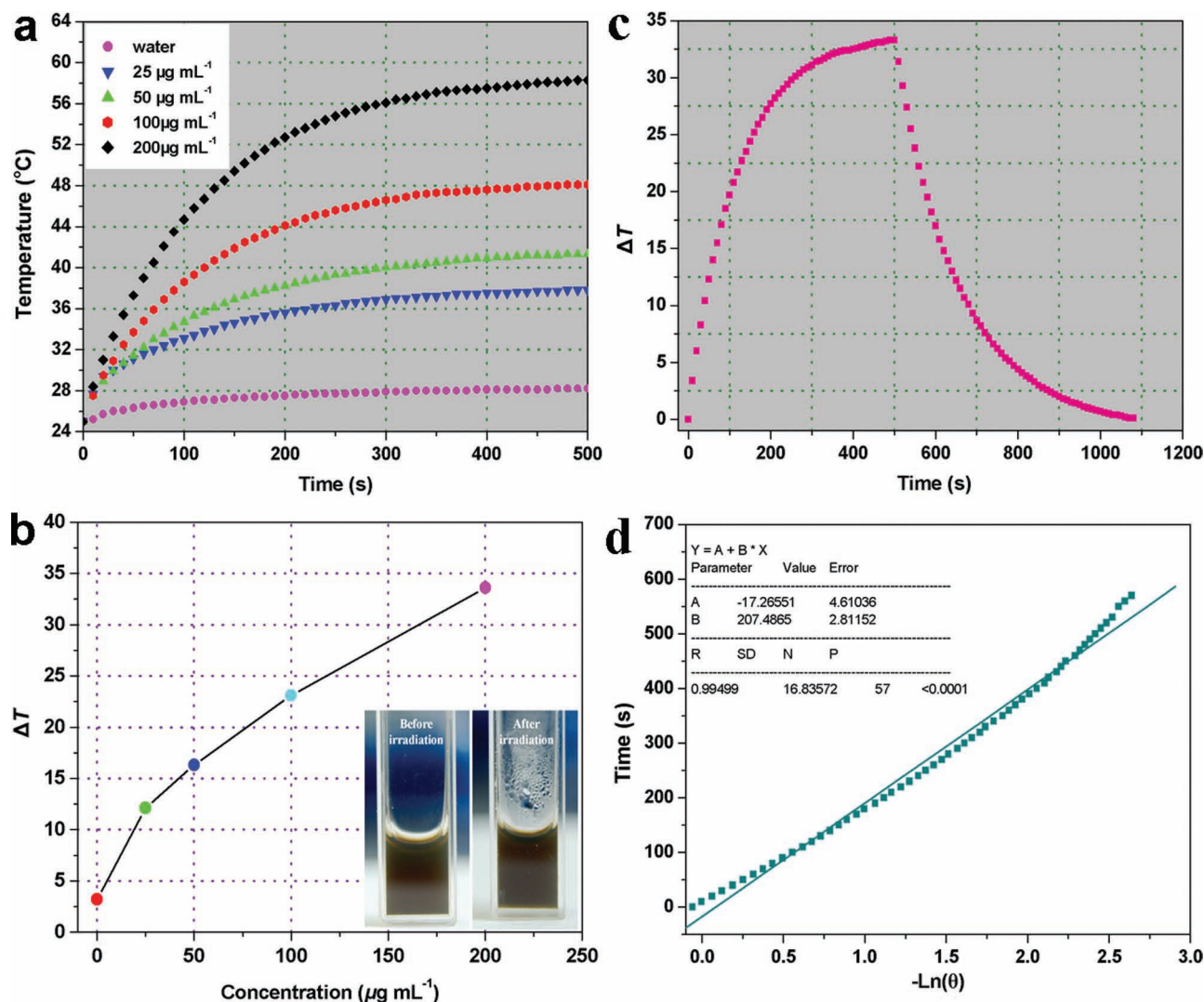
Figure 2. a) Temperature elevation of water and Dpa-melanin CNSs aqueous solutions with different concentrations as a function of irradiation time. b) Plot of temperature change (ΔT) over a period of 500 s versus the concentration of Dpa-melanin CNSs. The inset shows the photograph of Dpa-melanin CNSs dispersion in water before and after laser irradiation. c) The photothermal response of the Dpa-melanin CNSs aqueous solution (200 μg mL^{-1}) for 500 s with an NIR laser (808 nm, 2 W cm^{-2}) and then the laser was shut off. d) Linear time data versus $-\ln\theta$ obtained from the cooling period of Figure 2c.

led to a pronounced absorption extending from visible to NIR wavelengths.[18] To determine the NIR photoabsorption capability of Dpa-melanin CNSs, the molar extinction coefficient ε_{808} was evaluated (see Supporting Information for details), and was calculated to be 7.3×10^8 M^{-1} cm^{-1}. Although this value was a little lower than that of porphysomes ($\approx 10^9$ M^{-1} cm^{-1}), it was still much higher relative to many PTT agents reported elsewhere (Supporting Information, Table S1). The strong NIR absorption of Dpa-melanin CNSs makes them highly promising for photothermal cancer therapy. First, we evaluated their photothermal conversion capability. Dpa-melanin CNSs were dispersed in water at concentrations ranging from 25 to 200 μg mL^{-1}, and then irradiated with an 808 nm laser at 2 W cm^{-2} for 500 s. Pure water was used as a negative control. The temperatures

of all the Dpa-melanin CNSs samples increased with the irradiation time, and the temperature increased more rapidly with increasing the concentration of Dpa-melanin CNSs (**Figure 2**a). After irradiation for 500 s, the temperature of Dpa-melanin CNSs aqueous solution was increased by 33.6 °C at a concentration of 200 μg mL^{-1}, and water vapor droplets were observed on the wall of the cell (Figure 2b). In contrast, the temperature of pure water increased by only 3.2 °C. It has been demonstrated that the cancer cells can be killed after maintenance at 42 °C for 15–60 min; this duration can be shortened to 4–6 min for temperatures over 50 °C.[19] Assuming that the in vivo temperature of human body is 36 °C, after injection of Dpa-melanin CNSs, the tumor tissues can easily be heated to over 50 °C within 5 min after laser irradiation, efficiently killing the cancer cells.
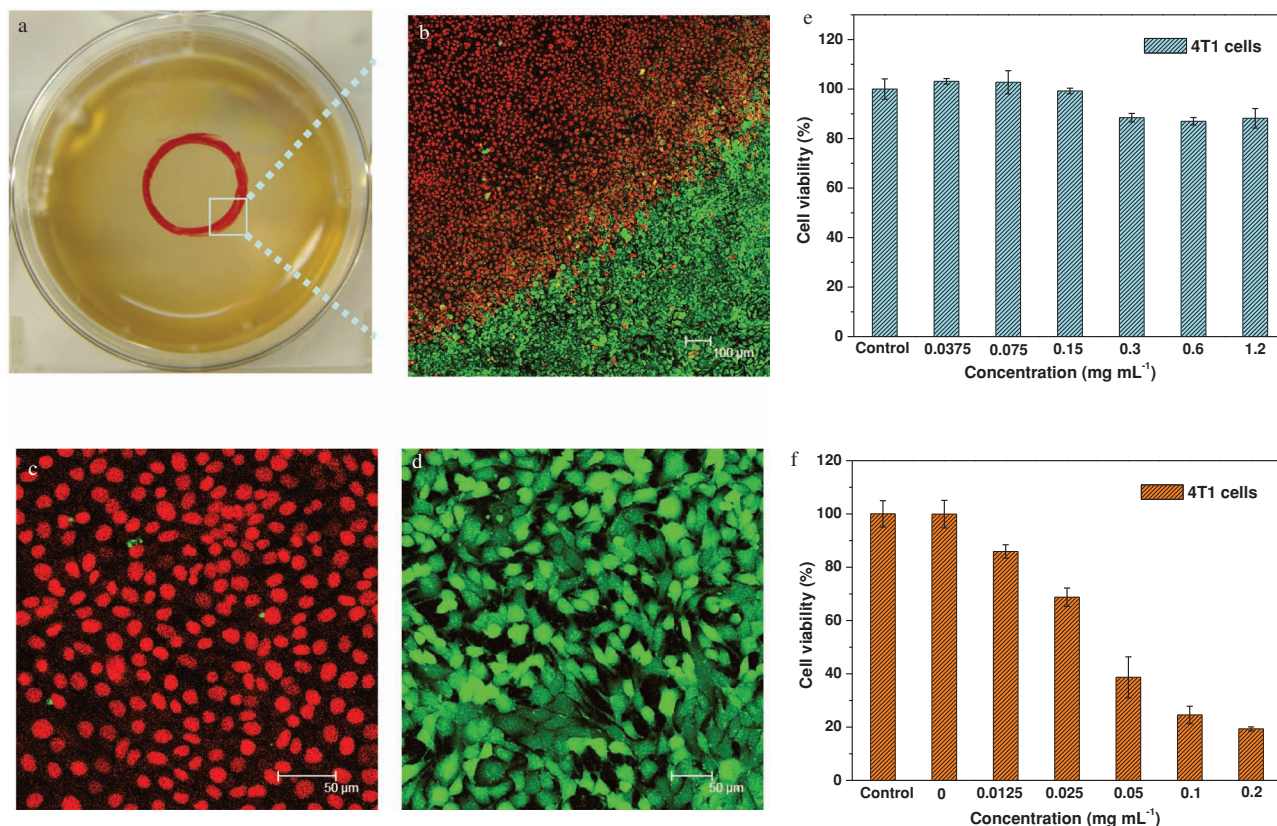
Figure 3. a) A digital photo of the 4T1 cell culture dish after incubation with Dpa-melanin CNSs. The red circle shows the laser spot. b–d) Confocal images of calcein AM (green, live cells) and propidium iodide (red, dead cells) co-stained 4T1 cells after laser irradiation. e) Cell viability of 4T1 cells after incubation with increased concentrations of Dpa-melanin CNSs. f) Cell viability of 4T1 cells treated with different concentrations of Dpa-melanin CNSs and laser irradiation (808 nm, 2 W cm^{-2}, 5 min).

Next, we measured the photothermal conversion efficiency (η) of Dpa-melanin CNSs. The η value was calculated (see Supporting Information for details) as follows:

$$\eta = \frac{h\,A\Delta T_{max} - Q_s}{I(1 - 10^{-A_\lambda})} \qquad (1)$$

where h is the heat transfer coefficient, A is the surface area of the container, ΔT_{max} is the temperature change of the Dpa-melanin CNSs solution at the maximum steady-state temperature, I is the laser power, A_λ is the absorbance of Dpa-melanin CNSs at 808 nm, Q_s is the heat associated with the light absorbance of the solvent, and η is the photothermal conversion efficiency. According to Equation 1, the η value of Dpa-melanin CNSs was determined to be 40%. Conversely, Au nanorods, which are widely used for cancer therapy, showed a much lower η value of 22% (Supporting Information, Figure S7). The higher η value of Dpa-melanin CNSs make them highly superior as a promising PTT agent.

To shed light on the possible reasons for such a higher photothermal conversion capability of Dpa-melanin CNSs, we investigated their absorption and photostability, which are two critical factors in determining the η values of PTT agents. As verified by resonance scattering analysis (Supporting Information, Figure S8), Dpa-melanin CNSs exhibited negligible resonance light scattering relative to Au nanorods in the NIR region, assuring their high photothermal conversion efficiency. We then proceeded to evaluate their photostability. Dpa-melanin CNSs and Au nanorods aqueous solutions were exposed to an 808 laser at 2 W cm^{-2} for 60 min, and their absorption and morphology were checked. No color change or absorption decrease was detected for Dpa-melanin CNSs. SEM image illustrated that Dpa-melanin CNSs maintained their morphology and size, indicating their high photostability (Supporting Information, Figure S9). In contrast, Au nanorods suffered significant loss of the NIR absorbance after laser irradiation resulting from their morphological change (melting) under local heating (Supporting Information, Figure S10). The excellent photostability further allowed Dpa-melanin CNSs to absorb more light and convert it into heat during the laser irradiation.

The high photothermal conversion efficiency of Dpa-melanin CNSs prompted us to evaluate their feasibility as a PTT agent for cancer therapy. Herein, 4T1 and HeLa cells were used as models of tumor tissues (**Figure 3**a–d, Supporting Information, Supporting Information, Figure S11–S13). The cells were incubated with Dpa-melanin CNSs for 30 min and then exposed to an 808 nm laser at 2 W cm^{-2} for 5 min. After treatment, the cells were stained with both calcein AM and propidium iodide (PI). Under excitation, a clear demarcation line between regions of live cells (green) and dead cells (red) was observed for both 4T1 and HeLa cells, and the majority of cells
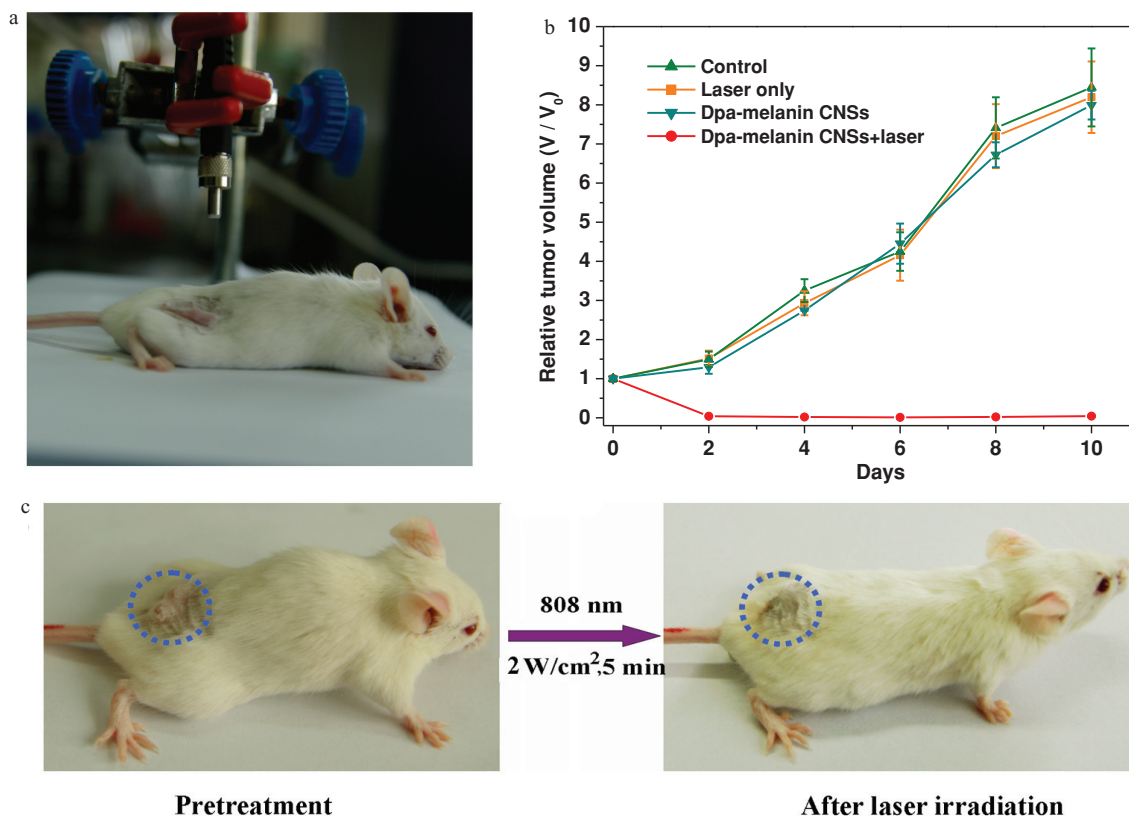
Figure 4. a) Photothermal therapy set-up showing laser and the 4T1 tumor-bearing mouse. b) Time-dependent tumor growth curves of the mice after different treatments. c) Digital photos of a 4T1 tumor-bearing mouse before and after photothermal therapy.

within the laser spot were killed. In contrast, cells treated with either Dpa-melanin CNSs or laser alone shown negligible cell death. These results suggested that Dpa-melanin CNSs could effectively kill the cancer cells only through the photothermal effect induced by NIR irradiation. We further quantitatively evaluated their photothermal cytotoxicity on cancer cells using an MTT (3-(4,5-dimethylthiazol-2-yl)-2,5-diphenyltetrazolium bromide) assay (Figure 3e,f). Taking 4T1 cells as an example, after 24 h of incubation with increasing concentrations of Dpa-melanin CNSs, neither the cell viability nor the proliferation in 4T1 cells was hindered by the presence of Dpa-melanin CNSs. Even at the highest tested dose of Dpa-melanin CNSs (1.2 mg mL^{-1}), cell viability still remained approximately 90%. However, upon laser irradiation, 4T1 cell viability decreased significantly as the concentration of Dpa-melanin CNSs increased, and less than 20% of cells remained alive at a concentration of 200 µg mL^{-1}. These findings demonstrated that Dpa-melanin CNSs hold great promise as an effective PTT agent for in vivo tumor therapy.

To assess their in vivo therapeutic potential, an aqueous solution of Dpa-melanin CNSs was injected intratumorally into several Balb/c mice bearing 4T1 tumors, and the tumors were then exposed to an 808 nm laser at 2 W cm^{-2} for 5 min. Most of the tumor tissue was necrotic after treatment; shrunken malignant cells, cytoplasmic acidophilia, and corruption of the tumor extracellular matrix were observed (Supporting Information, Figure S14). Conversely, tumor tissues from control animals

and mice that received laser only remained normal. During ten days of observation, the tumors on injected mice were ablated after photothermal treatment without regrowth or with rather slow growth. In contrast, tumors in the control animals and mice that received laser treatment alone continued to grow rapidly, and all of these mice had to be euthanized after ten days (**Figure 4**).

Indeed, Dpa-melanin CNSs can provide an important platform for in vivo applications, since their surface can be easily modified with thiol- and amino-terminated molecules through Michael addition or Schiff base reaction, and thus facilitated the loading of conjugates with other interesting biofunctionalities. To demonstrate their versatility, we fabricated Gd-DTPA-modified Dpa-melanin CNSs and further investigated their applications in magnetic resonance imaging and therapy of tumor in vivo. The resultant agent possessed a relaxivity value of 6.9 mM^{-1} s^{-1}, superior to the commercial Magnevist (Supporting Information, Figure S15). After intravenous injection, The T_1 signals from tumor sites showed a trend of increase and became quite strong at 24 h. Their accumulation in tumor was 5.7% ID g^{-1} (**Figure 5** and Supporting Information, Figure S16). Upon laser irradiation, the tumor was also destroyed (Supporting Information, Figure S17).

Dpa-melanin CNSs are highly suited for in vivo applications because Dpa-melanin is widely distributed throughout the human body and it can be physically metabolized, which can effectively reduce potential serious adverse effects in patients.
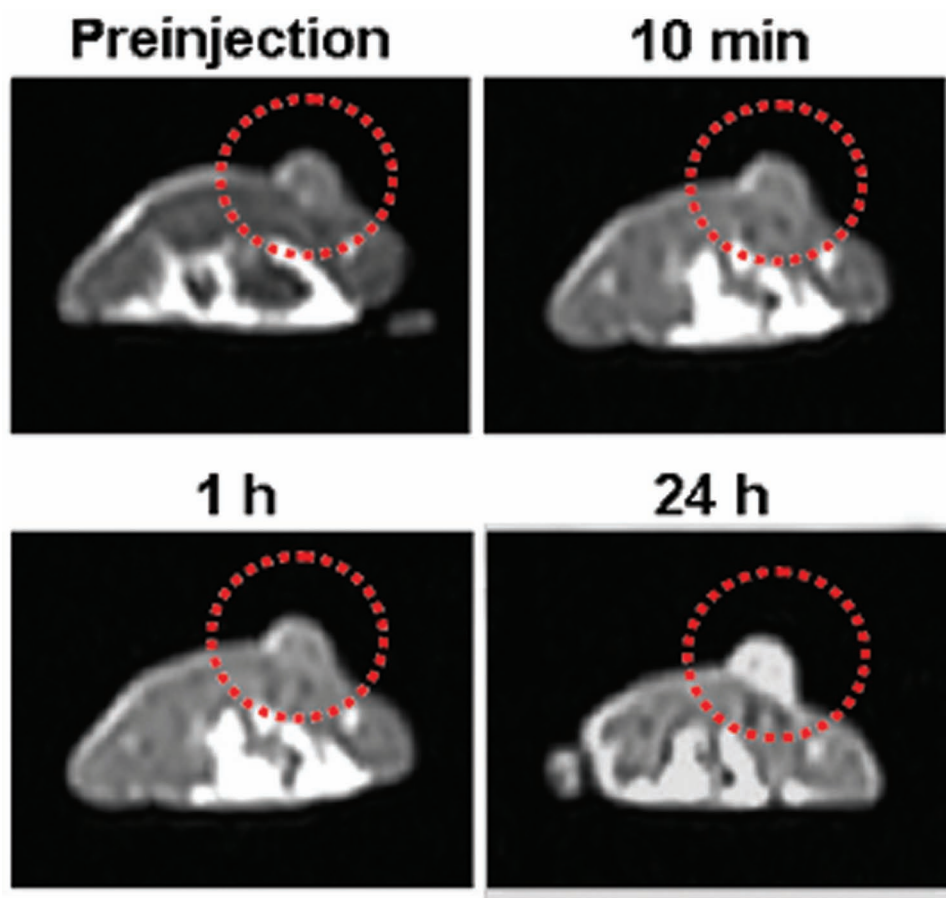
Figure 5. In vivo T_1-weighted MR images of the 4T1-tumor bearing mouse before and after intravenous injection of the Gd-DTPA-modified Dpa-melanin CNSs solution. The red circles point the tumor sites.

In our preliminary observations, Dpa-melanin CNSs lost their absorbance coupled with color fading in the presence of hydrogen peroxide (Supporting Information, Figure S18), an endogenous molecule produced by reduced nicotinamide adenine dinucleotide phosphate (NADPH) oxidases, which widely exist in phagocytes and many organs.[20] This finding suggested that Dpa-melanin CNSs were biodegradable in vivo. Next, we proceeded to assess their potential in vivo toxicity. The median lethal dose (LD_{50}) is a standardized measure used to evaluate the acute toxicity of agents. Here, Dpa-melanin CNSs had a LD_{50} value (intravenous injection) as high as 483.95 mg kg^{-1} with a 95% confidence interval of 400.22 to 585.19 mg kg^{-1}. This dose was nearly five hundred times higher than the dose used for photothermal therapy in this work.

Lastly, the long-term toxicity of Dpa-melanin CNSs was investigated. After intravenous injection of a single dose of Dpa-melanin CNSs, the rats remained healthy over one-month period, no abnormalities in eating, drinking, grooming, activity, exploratory behaviour, urination, or neurological status were observed. The body weight of the treated group gradually increased in a manner similar to that of the control group (Supporting Information, Figure S19). After one month, the rats were euthanized and several susceptible organs were stained with hematoxylin and eosin (H&E) for histological analysis (Supporting Information, Figure S20a). No tissue damage or any other adverse effect associated with the administration of Dpa-melanin CNSs was detected. The five important hepatic indicators – alkaline phosphatase (ALP), alanine transaminase (ALT), aspartate transaminase (AST), total protein (TP) and albumin/globin ratio (A/G) – fell within normal ranges and revealed no sign of liver injury. Complete blood tests showed no obvious interference with the physiological regulation of haem or immune response (Supporting Information, Figure S20b).

In summary, we have successfully presented a new generation of photothermal therapeutic agent based on biopolymer Dpa-melanin CNSs. Dpa-melanin CNSs were completely composed of Dpa-melanin that was widely distributed throughout the human body. This could effectively avoid serious adverse effects associated with the long-term retention of foreign substances in patients. Dpa-melanin CNSs could be easily prepared and well dispersed in aqueous media with high colloidal stability. Furthermore, they showed strong NIR absorption and high photothermal conversion efficiency, and could efficiently kill cancer cells and suppress tumor growth without damaging healthy tissues. Toxicity experiments confirmed their excellent biocompatibility. They possessed a high LD_{50} value and were biodegradable. Finally, Dpa-melanin CNSs could react with thiol- and amino-terminated molecules, which facilitated the design of multifunctional nanomedical platforms for simultaneous diagnosis and therapy of cancer.

Experimental Section

Animal care and handing procedures were in agreement with the guidelines of the Regional Ethics Committee for Animal Experiments.

Supporting Information

Supporting Information is available from the Wiley Online Library or from the author.

Acknowledgements

Materials
Views

www.MaterialsViews.com

ADVANCED
MATERIALS

www.advmat.de

COMMUNICATION

[1] D. Yoo, J.-H. Lee, T.-H. Shin, J. Cheon, *Acc. Chem. Res.* **2011**, *44*, 863.

[2] R. Bardhan, S. Lal, A. Joshi, N. Halas, *Acc. Chem. Res.* **2011**, *44*, 936.

[3] F. M. Kievit, M. Q. Zhang, *Acc. Chem. Res.* **2011**, *44*, 853.

[4] A. Vogel, V. Venugopalan, *Chem. Rev.* **2003**, *103*, 577.

[5] C. P. Nolsøe, S. Torp-Pedersen, F. Burcharth, T. Horn, S. Pedersen, N. E. Christensen, E. S. Olldag, P. H. Andersen, S. Karstrup, T. Lorentzen, *Radiology* **1993**, *187*, 333.

[6] S. Lal, S. E. Clare, N. J. Halas, *Acc. Chem. Res.* **2008**, *41*, 1842.

[7] W. I. Choi, J.-Y. Kim, C. Kang, C. C. Byeon, Y. H. Kim, G. Tae, *ACS Nano* **2011**, *5*, 1995.

[8] a) S. Wang, K.-J. Chen, T.-H. Wu, H. Wang, W.-Y. Lin, M. Ohashi, P.-Y. Chiou, H.-R. Tseng, *Angew. Chem. Int. Ed.* **2010**, *49*, 3777; b) X. H. Huang, I. H. El-Sayed, W. Qian, M. A. El-Sayed, *J. Am. Chem. Soc.* **2006**, *128*, 2115; c) W.-S. Kuo, C.-N. Chang, Y.-T. Chang, M.-H. Yang, Y.-H. Chien, S.-J. Chen, C.-S. Yeh, *Angew. Chem. Int. Ed.* **2010**, *49*, 2711; d) H. Liu, D. Chen, L. Li, T. Liu, L.Tan, X. Wu, F. Tang, *Angew. Chem. Int. Ed.* **2011**, *50*, 891; e) W. Dong, Y. Li, D. Niu, Z. Ma, J. Gu, Y. Chen, W. Zhao, X. Liu, C. Liu, J. Shi, *Adv. Mater.* **2011**, *23*, 5392; f) H. Ke, J. Wang, Z. Dai, Y. Jin, E. Qu, Z. Xing, C. Guo, X. Yue, J. Liu, *Angew. Chem. Int. Ed.* **2011**, *50*, 3017; g) J. Chen, D. Wang, J. Xi, L. Au, A. Siekkinen, A. Warsen, Z.-Y. Li, H. Zhang, Y. Xia, X. Li, *Nano Lett.* **2007**, *5*, 1318; h) K.-W. Hu, C.-C. Huang, J.-R. Hwu, W.-C. Su, D.-B. Shieh, C.-S. Yeh, *Chem. Eur. J.* **2008**, *14*, 2956; i) X. Huang, S. Tang, X. Mu, Y. Dai, G. Chen, Z. Zhou, F. Ruan, Z. Yang, N Zheng, *Nat. Nanotechnol.* **2011**, *6*, 28.

[9] a) Q. Tian, M. Tang, Y. Sun, R. Zou, Z. Chen, M. Zhu, S. Yang, J. Wang, J. Wang, J. Hu, *Adv. Mater.* **2011**, *23*, 3542; b) C. M. Hessel,

[10] a) K. Yang, S. Zhang, G. Zhang, X. Sun, S.-T. Lee, Z. Liu, *Nano Lett.* **2010**, *10*, 3318; b) J. T. Robinson, S. M. Tabakman, Y. Liang, H. Wang, H. S. Casalongue, D. Vinh, H. Dai, *J. Am. Chem. Soc.* **2011**, *133*, 6825; c) H. K. Moon, S. H. Lee, H. C. Choi, *ACS Nano* **2009**, *3*, 3707.

[11] J. Yang, J. Choi, D. Bang, E. Kim, E.-K. Lim, H. Park, J.-S. Suh, K. Lee, K.-H. Yoo, E.-K. Kim, Y.-M. Huh, S. Haam, *Angew. Chem. Int. Ed.* **2011**, *50*, 441.

[12] a) A. Nel, T. Xia, L. Madler, N. Li, *Science* **2006**, *311*, 622; b) S. Sharifi, S. Behzadi, S. Laurent, M. L. Forrest, P. Stroeve, M Mahmoudi, *Chem. Soc. Rev.* **2012**, *41*, 2323.

[13] a) J. F. Lovell, C. S. Jin, E. Huynh, T. D. MacDonald, W. Cao, G. Zheng, *Angew. Chem. Int. Ed.* **2012**, *51*, 2429; b) J. F. Lovell, C. S. Jin, E. Huynh, H. Jin, C. Kim, J. L. Rubinstein, W. C. W. Chan, W. Cao, L. V. Wang, G. Zheng, *Nat. Mater.* **2011**, *10*, 324.

[14] a) J. D. Simon, *Acc. Chem. Res.* **2000**, *33*, 307; b) Y. Liu, J. D. Simon, *Pigment Cell Res.* **2003**, *16*, 606.

[15] a) Y. L. Liu, K. L. Ai, J. H. Liu, Y. Q. Hai, Y. Y. He, L. H. Lu, *Angew. Chem. Int. Ed.* **2012**, *51*, 1437; b) K. L. Ai, Y. L. Liu, J. H. Liu, Y. Q. Hai, Y. Y. He, L. H. Lu, *Adv. Mater.* **2011**, *23*, 4886; c) M. T. Zhu, G. J. Nie, H. Meng, T. Xia, A. Nel, Y. L. Zhao, *Acc. Chem. Res. DOI: 10.1021/ar300031y*; d) Y. L. Liu, K. L. Ai, L. H. Lu, *Acc. Chem. Res.* **2012**, *45*, 1817.

[16] a) M. S. Blois, J. E. Maling, A. B. Zahlan, *Biophys. J.* **1964**, *4*, 471; b) O. Z. Fisher, B. L. Larson, P. S. Hill, D. Graupner, M.-T. Nguyen-Kim, N. S. Kehr, L. D. Cola, R. Langer, D. G. Anderson, *Adv. Mater.* **2012**, *24*, 3032.

[17] a) M. C. Peter, H. Forsfer, *Angew. Chem. Int. Ed.* **1989** *28*, 741; b) S. A. Centeno, J. Shamir, *J. Mol. Struct.* **2008**, *873*, 149.

[18] H. Xu, X. Liu, D. Wang, *Chem. Mater.* **2011**, *23*, 5105.

[19] R. W. Y. Habash, R. Bansal, D. Krewski, H. T. Alhafid, *Crit. Rev. Biomed. Eng.* **2006**, *34*, 459.

[20] A. C. Cave, A. C. Brewer, A. Narayanapanicker, R. Ray, D. J. Grieve, S. Walker, A. M. Shah, *Antioxid. Redox Signaling* **2006**, *8*, 691.